

# UC Davis

## UC Davis Previously Published Works

### Title

Mid-gestation serum lipidomic profile associations with spontaneous preterm birth are influenced by body mass index

### Permalink

<https://escholarship.org/uc/item/7jt6v740>

### Journal

PLOS ONE, 15(11)

### ISSN

1932-6203

### Authors

Borkowski, Kamil  
Newman, John W  
Aghaeepour, Nima  
[et al.](#)

### Publication Date

2020

### DOI

10.1371/journal.pone.0239115

Peer reviewed

## RESEARCH ARTICLE

# Mid-gestation serum lipidomic profile associations with spontaneous preterm birth are influenced by body mass index

Kamil Borkowski<sup>1\*</sup>, John W. Newman<sup>1,2,3</sup>, Nima Aghaeeepour<sup>4,5,6</sup>, Jonathan A. Mayo<sup>5</sup>, Ivana Blazenović<sup>1</sup>, Oliver Fiehn<sup>1</sup>, David K. Stevenson<sup>5</sup>, Gary M. Shaw<sup>5</sup>, Suzan L. Carmichael<sup>5</sup>

**1** West Coast Metabolomic Center, Genome Center, University of California-Davis, Davis, CA, United States of America, **2** United States Department of Agriculture-Agriculture Research Service-Western Human Nutrition Research Center, Davis, CA, United States of America, **3** Department of Nutrition, University of California-Davis, Davis, CA, United States of America, **4** Department of Anesthesiology, Pain, and Perioperative Medicine, Stanford University School of Medicine, Stanford, CA, United States of America, **5** Department of Pediatrics, Stanford University School of Medicine, Stanford, CA, United States of America, **6** Department of Biomedical Data Sciences, Stanford University School of Medicine, Stanford, CA, United States of America

\* [kborkowski@ucdavis.edu](mailto:kborkowski@ucdavis.edu)



## OPEN ACCESS

**Citation:** Borkowski K, Newman JW, Aghaeeepour N, Mayo JA, Blazenović I, Fiehn O, et al. (2020) Mid-gestation serum lipidomic profile associations with spontaneous preterm birth are influenced by body mass index. PLoS ONE 15(11): e0239115. <https://doi.org/10.1371/journal.pone.0239115>

**Editor:** Francisco J. Schopfer, University of Pittsburgh, UNITED STATES

**Received:** March 10, 2020

**Accepted:** August 31, 2020

**Published:** November 17, 2020

**Copyright:** This is an open access article, free of all copyright, and may be freely reproduced, distributed, transmitted, modified, built upon, or otherwise used by anyone for any lawful purpose. The work is made available under the [Creative Commons CC0](https://creativecommons.org/licenses/by/4.0/) public domain dedication.

**Data Availability Statement:** The data in this study is third-party data obtained from the California Biobank Program. California law prohibits us from uploading the raw metabolomic data generated in this study to any public repository. As allowed under our IRB, we have included aggregate data in the paper's Supporting Information as [S2](#) and [S3](#) Tables. If researchers are interested in seeking data specimens such as those used in this research they are encouraged to contact CBP directly via their web-site and following the guidance for accessing samples at <https://www.cdph.ca.gov/>

## Abstract

Spontaneous preterm birth (sPTB) is a major cause of infant morbidity and mortality. While metabolic changes leading to preterm birth are unknown, several factors including dyslipidemia and inflammation have been implicated and paradoxically both low (<18.5 kg/m<sup>2</sup>) and high (>30 kg/m<sup>2</sup>) body mass indices (BMIs) are risk factors for this condition. The objective of the study was to identify BMI-associated metabolic perturbations and potential mid-gestation serum biomarkers of preterm birth in a cohort of underweight, normal weight and obese women experiencing either sPTB or full-term deliveries (n = 102; n = 17/group). For this purpose, we combined untargeted metabolomics and lipidomics with targeted metabolic profiling of major regulators of inflammation and metabolism, including oxylipins, endocannabinoids, bile acids and ceramides. Women who were obese and had sPTB showed elevated oxidative stress and dyslipidemia characterized by elevated serum free fatty acids. Women who were underweight-associated sPTB also showed evidence of dyslipidemia characterized by elevated phospholipids, unsaturated triglycerides, sphingomyelins, cholesteryl esters and long-chain acylcarnitines. In normal weight women experiencing sPTB, the relative abundance of 14(15)-epoxyeicosatrienoic acid and 14,15-dihydroxyeicosatrienoic acids to other regioisomers were altered at mid-pregnancy. This phenomenon is not yet associated with any biological process, but may be linked to estrogen metabolism. These changes were differentially modulated across BMI groups. In conclusion, using metabolomics we observed distinct BMI-dependent metabolic manifestations among women who had sPTB. These observations suggest the potential to predict sPTB mid-gestation using a new set of metabolomic markers and BMI stratification. This study opens the door to further investigate the role of cytochrome P450/epoxide hydrolase metabolism in sPTB.

[Programs/CFH/DGDS/Pages/cbp/default.aspx](https://doi.org/10.1371/journal.pone.0239115). The authors had no special access privileges to the data, and other researchers can access the data following the same application process.

**Funding:** This research was supported by the March of Dimes Foundation Prematurity Research Center at Stanford University School of Medicine project 22-FY18-808 (GMS, DKS); the Hess Research Fund award HAESD at Stanford University (DKS); the Lucile Packard Foundation for Children's Health; the Stanford Child Health Research Institute, the National Institutes of Health project UL1-TR001085 (SLC, GMS, DKS); and the NIH West Coast Metabolomics Center NIH U24 DK097154 (OF, JWN) as a 2015 Pilot Project (SLC). Additional support was provided by USDA Projects 2032-51530-022-00D and 2032-51530-025-00D (JWN). The USDA is an equal opportunity employer and provider.

**Competing interests:** The authors have declared that no competing interests exist.

**Abbreviations:** BMI, body mass index; COX, Cyclooxygenase; CYP, Cytochrome P450; DiHETrE, Dihydroxyecosatrienoic acid; DiHOME, Dihydroxy-octadeca(mono)eneoic acid; EpETrE, Epoxyecosatrienoic acid; FTB, Full-term birth; HETE, Hydroxyecosatetraenoic acid; IL, Interleukin; LOX, Lipoxygenase; MMPs, Matrix metalloproteinases; PUFA, Polyunsaturated fatty acids; sE, Soluble epoxide hydrolase; sPTB, Spontaneous preterm birth.

## Introduction

Preterm birth, i.e. delivery at <37wk gestation, is a major cause of infant morbidity and mortality, and accounts for 1 in 10 or ~400,000 births per year in the United States and ~11% of births worldwide or ~15 million births annually [1]. Part of the overall occurrence of preterm birth can be attributed to maternal or fetal conditions requiring medical intervention to facilitate delivery before term. However, risk factors and etiology of the largest population burden of preterm birth, spontaneous preterm birth (sPTB), remain largely unexplained [2]. As parturition is associated with an exquisitely regulated inflammatory process that promotes uterine contractility, cervical maturation and amniotic membrane rupture, pathophysiological priming of the inflammatory response by a variety of systemic stressors may increase the likelihood of sPTB [3, 4]. Vaginal infection, chronic inflammation, and inflammation-associated conditions like obesity and hypertension place a pregnancy at risk [5–7]. In fact early- to mid-gestation markers of low grade systemic inflammation, including increased pro-inflammatory cytokines interleukin (IL)-6, IL-8 and c-reactive protein and decreased anti-inflammatory IL-10, have been detected in women experiencing sPTB [8–11]. Notably, body mass indices (BMIs) for obesity (>30 kg/m<sup>2</sup>) and underweight (<18.5 kg/m<sup>2</sup>) relative to the normal range increase risks of sPTB [12–16], and the association of BMI with inflammation also exhibits a “U-shaped” behavior [17].

The inflammatory response is a multifaceted and coordinated system of interacting proteins and small molecule mediators with variability derived from both environmental and genetic influences [18]. Mechanistic associations between inflammation and sPTB have largely focused on protein level changes including cytokines [16], matrix metalloproteinases (MMPs) [19, 20], tissue inhibitors of MMPs [20], and tissue plasminogen activator [21]. Metabolomic investigation of circulating metabolites can provide a broader overview of changes in metabolism [22, 23] and inflammatory responses [24, 25]. Recent efforts have probed the metabolome for biomarkers of sPTB and clues to the etiology of the condition [26, 27]. While few of these studies have investigated maternal blood, those that have observed consistent differences in circulating lipids, with some reporting lipid mediator differences in plasma that can predict sPTB sub-type [26–28]. Among lipid mediators of inflammation, oxylipins, endocannabinoids, bile acids, and ceramides have each been implicated in the pathologies associated with preterm delivery [28–33]. Importantly, while the serum levels of these metabolites increase with BMI [34–36], this increase is associated with poor metabolic health (i.e. diabetes status) rather than obesity [37].

We designed the current study to specifically investigate BMI-associated metabolic perturbations and potential mid-gestational serum biomarkers for their associations with sPTB-risk in a cohort of underweight, normal weight, and obese women. To accomplish this goal, we have combined untargeted metabolomics and lipidomics with targeted metabolic profiling of non-esterified oxylipins, endocannabinoids, bile acids, ceramides and polyunsaturated fatty acids (PUFA) in mid-gestation serum samples.

## Materials and methods

### Subjects

Serum samples were collected from pregnant women in the gestational timing of 15–17 weeks by the California Biobank Program. This Biobank stores serum remaining after the California Prenatal Screening Program has conducted mid-gestation screening for fetal conditions such as trisomies and neural tube defects from women residing in selected CA counties: Orange, San Diego, Fresno, Madera, Merced, San Benito, Monterey, Kings, Tulare, Inyo, and Mono.

Hospital discharge information from 2007 to 2011 were used to identify women with collected samples that were appropriate for the study. We identified nulliparous women who were linked to singleton livebirths birth certificate data provided by the Office of Statewide Health Planning and Development. Inclusion criteria were based on BMI [underweight (<18.5 kg/m<sup>2</sup>); normal (18.5–24.9 kg/m<sup>2</sup>); and obese (≥30 kg/m<sup>2</sup>)] and gestational age (sPTB <31 weeks; full-term birth (FTB) >37 weeks). BMI was based on self-reported weight and height and gestational age on best obstetric estimate, both as reported on the birth certificate. A review of self-reported maternal pre-pregnancy weight and weight change found that misclassification generally does not induce bias in associations with perinatal outcomes [38]. To reduce heterogeneity among all preterm births, we restricted the study to sPTB, i.e., those with preterm premature rupture of membranes, premature labor, or tocolytics based on information from the birth certificate or ICD-9 codes from the delivery hospitalization record. A list of births meeting these inclusion criteria was sent to the Biobank program to identify births with available serum samples and randomly select a sub-set from the following groups for our study: underweight sPTB (n = 288); underweight FTB (n = 11,430); normal weight sPTB (n = 366); normal weight FTB (n = 115,907); obese sPTB (n = 263); obese FTB (n = 28,510). From the available samples, we randomly selected 17 from each group for the current analysis. The sample group criteria and numbers selected were based in part on sample availability and budgetary constraints. Demographic information was derived from the birth certificate. Maternal race/ethnicity was categorized as non-Hispanic White, non-Hispanic Black, Asian, Pacific Islander, Hispanic, and missing. Maternal education was categorized as some high school or less, high school graduate or equivalent, some college, college degree or more, and missing. Maternal age (years) was included as a continuous variable. The study was approved by the California Committee for the Protection of Human Subjects, protocol number 15-01-1835. Data were analyzed anonymously.

### Serum targeted metabolomics

Quantitative targeted metabolomic profiling was performed using UPLC-MS/MS based methods in the presence of isotopically labeled or rare internal standards at the West Coast Metabolomics Center Lipid Mediators Research Laboratory (<https://metabolomics.ucdavis.edu/research-labs/newman-laboratory-for-lipid-mediators>). A complete list of extraction surrogates and their exact concentrations are presented in the **S1 Table**.

Oxylipins, endocannabinoids, PUFA and bile acids from 40 μL of serum were quantified after methanol/acetonitrile (1:1 v/v) protein precipitation [39]. Briefly, 40 μL of serum was mixed with 5 μL BHT/EDTA (1:1 methanol:water), 10 μL of 0.5 μM deuterated oxylipin, endocannabinoid and PUFA surrogates and 20 μL of 1 μM deuterated bile acid surrogates in methanol. Next, serum was homogenized by the vigorous addition of 200 μL of 1:1 methanol:acetonitrile containing 100 nM 1-cyclohexyl ureido, 3-dodecanoic acid (CUDA; Sigma, St. Louis MO) and 1-phenyl ureido 3-hexanoic acid (PUHA; kind gift from Dr. B.D. Hammock, University of California Davis). The homogenate was centrifuged at 15000 rcf for 10 min and the supernatant was filtered at 0.1 μm PVDF membranes (MiliporeSigma, Burlington, MA) at 1000 rcf for 5 min and collected for mass spectrometry analysis.

NS-ceramides were isolated and quantified using minor modifications of published procedures [40, 41]. Briefly, 100 μL of serum was mixed with 5 μL BHT/EDTA (1:1 methanol:water), 10 μL of 1 μM odd-chain length ceramide surrogates, and mixed with 410 μL of 2-propanol, followed by 520 μL of cyclohexane. Organic and aqueous phase splits were accomplished with the addition of 413 μL LC-MS grade water and 57 μL of 1 M ammonium acetate, and centrifugation at 10,000 rcf for 5 min. The upper organic phase was retrieved and dried

under vacuum at 15 Hg for 10 min and residues were reconstituted in 100  $\mu$ L of 1:1 methanol:acetonitrile containing 100 nM CUDA and PUHA.

Residues in extracts were separated on a 2.1 mm x 150 mm, 1.7  $\mu$ m BEH C18 column (Waters, Milford, MA) for oxylipins and endocannabinoids analysis, 2.1 mm x 100 mm, 1.7  $\mu$ m BEH C18 column (Waters) for bile acids analysis and 2.1 mm x 150 mm, 1.7  $\mu$ m BEH C8 column (Waters) for ceramides analysis and detected by electrospray ionization with multi reaction monitoring on a API 6500 QTRAP (Sciex; Redwood City, CA) and quantified against 7–9 point calibration curves of authentic standards using modifications of previously reported methods [37, 42]. A complete list of metabolites together with groups means and p-values are provided in the [S2 Table](#).

### Serum untargeted metabolomics

Semi-quantitative, untargeted metabolomic profiling was performed in the West Coast Metabolomics Center Central Services Core (<https://metabolomics.ucdavis.edu/core-services/assays-and-services>) as previously described to provide semiquantitative analysis of complex lipids and biogenic amines [43, 44]. Serum lipids were extracted from 40  $\mu$ L of serum using biphasic solvent system of 300  $\mu$ L of cold methanol containing odd chain and deuterated lipid internal standards: [LPE(17:1), LPC(17:0), PC(12:0/13:0), PE(17:0/17:0), PG(17:0/17:0), d7-cholesterol, SM(d18:1/17:0), Cer(d18:1/17:0), sphingosine(d17:1), DG(12:0/12:0/0:0), DG(18:1/2:0/0:0), and d5-TG-(17:0/17:1/17:0)], 1000  $\mu$ L methyl tertbutyl ether (MTBE) containing CE(22:1) internal standard, and 250  $\mu$ L of water. Lipid standards were purchased from Avanti Polar Lipids (Alabaster, AL USA). A 100  $\mu$ L aliquot of the organic phase was dried under vacuum and subsequently reconstituted in 100  $\mu$ L of methanol/toluene (9:1, v/v) containing CUDA (150 ng/mL) as an internal standard prior to LC-MS analysis. Biogenic amines were retrieved from the aqueous phase of the lipid extraction procedure. Samples were dried under the vacuum and rinsed with (1:1, v/v) acetonitrile: water to remove proteins and dried again under vacuum. Samples were reconstituted for Hydrophilic Interaction Liquid Chromatography (HILIC) mass spectrometry analysis in (80:20, v/v) acetonitrile:water solution containing CUDA (150 ng/mL) and deuterated internal standards. All measurements were carried out on a Thermo Q Exactive mass spectrometer. For complex lipids, 1  $\mu$ L of extracts were separated on a Waters Acquity UPLC CSH C18 column (100  $\times$  2.1 mm; 1.7  $\mu$ m) coupled to an Acquity UPLC CSH C18 VanGuard precolumn (5  $\times$  2.1 mm; 1.7  $\mu$ m). The column was maintained at 65°C at a flow rate of 0.6 mL/min. The positive ionization mobile phases consisted of (A) acetonitrile:water (60:40, v/v) with ammonium formate (10 mM) and formic acid (0.1%) and (B) 2-propanol:acetonitrile (90:10, v/v) with ammonium formate (10 mM) and formic acid (0.1%). The negative ionization mobile phases consisted of (A) acetonitrile: water (60:40, v/v) with ammonium formate (10 mM) and (B) 2-propanol: acetonitrile (90:10, v/v) with ammonium formate (10 mM). The separation was conducted under the following gradient: 0 min 15% B; 0–2 min 30% B; 2–2.5 min 48% B; 2.5–11 min 82% B; 11–11.5 min 99% B; 11.5–12 min 99% B; 12–12.1 min 15% B; 12.1–15 min 15% B. For biogenic amines, hydrophilic interaction liquid chromatography (HILIC)-Q Exactive MS/MS data acquisition was performed. 1  $\mu$ L of samples were separated on a Waters Acquity UPLC BEH Amide column (150  $\times$  2.1 mm; 1.7  $\mu$ m) coupled to an Acquity UPLC BEH Amide VanGuard precolumn (5  $\times$  2.1 mm; 1.7  $\mu$ m). The column was maintained at 45°C with a flow rate of 0.4 mL/min. The mobile phases consisted of (A) water with ammonium formate (10 mM) and formic acid (0.125%) and (B) acetonitrile: water (95:5, v/v) with ammonium formate (10 mM) and formic acid (0.125%). The separation was conducted under the following gradient: 0 min 100% B; 0–2 min 100% B; 2–7.7 min 70% B; 7.7–9.5 min 40% B; 9.5–10.25 min 30% B; 10.25–12.75 min 100%

B; 12.75–17 min 100% B. The Q Exactive MS was operated using positive and negative mode electrospray ionization (ESI HILIC) with the following parameters: Mass range, 60–900 m/z; Sheath gas flow rate, 60; Aux gas flow rate, 25; Sweep gas flow rate, 2; Spray Voltage (kV) 3.6; Capillary temp, 300°C; S-lens RF level, 50; Aux gas heater temp, 370°C. Full MS parameters: Microscans—1; Resolution—60,000; AGC target - 1e6; Maximum IT - 100ms; Number of scans—1; Spectrum data type—Centroid. Data dependent MS2 parameters: Microscans—1; Resolution—15,000; AGC target - 1e5; Maximum IT—50 ms; Loop count—4; MSX count—1; TopN—4; Isolation Window—1.0 m/z; Isolation offset—0.0 m/z; (N)CE / stepped (N)CE—20, 30, 40; Spectrum data type—Centroid. The LC-MS/MS data were analyzed by MS-DIAL software [45]. Metabolite annotations were achieved using a combination of different tools. Metabolomics Standards Initiative (MSI) has defined levels of compound annotation which we applied in this paper [46]. On MSI level 1 we used a HILIC-MS/MS library of 1,400 authentic standards including retention time, precursor mass and MS/MS spectra. All spectra, retention times and chromatography conditions are freely available at MassBank of North America (<http://massbank.us>). Search windows were used as follows: 0.1 min RT tolerance (for the alignment of peaks), 0.01 Da tolerance for the precursor masses and 0.05 Da tolerance for the MS/MS spectral matching. Similarly, we used lipid retention times and MS/MS spectra for lipidomics identifications [47]. On MSI level 2, we annotated compounds that did not trigger MS/MS fragmentations in data dependent mode but that were still identified based on accurate mass and retention time using the HILIC-MS/MS library in addition to manually curated lipid retention times. For MSI level 3 annotations, we annotated compounds based on the MSI information only using MS-DIAL software which has integrated Seven Golden Rules within [45, 48].

## Statistical analysis

All statistical tests were performed using JMP Pro 14.1 (JMP, SAS institute, Cary, NC). Prior to analysis, metabolite outliers were detected and removed using the robust Huber M test and missing data were imputed using multivariate normal imputation. Data imputation was performed to facilitate multivariate data analysis but did not significantly change results observed with univariate analysis (e.g. t-tests). The total of 1.14% of the data were imputed with a number of missing values in a single variable not exceeding 25%. Data were then transformed to obtain normal distributions using Johnson's transformation. All analyses were stratified by BMI and metabolite data were adjusted for maternal age and race/ethnicity. Our primary objective was to evaluate BMI—specific metabolic perturbation related to sPTB in underweight, normal weight and obese BMI categories, and both sample collection and analyses were designed in a BMI-stratified fashion. Secondary analyses were performed to verify the appropriateness of the stratification approach. A factorial analysis was used to evaluate interaction between BMI categories and birth groups, as well as a general birth group effect. This model included BMI category, birth category, BMI x birth category interaction as the fixed effect and mother's age as a covariate. Further, ANCOVA was used to evaluate metabolite mean differences between FTB and sPTB while evaluating the potential use of BMI as either a continuous or categorical covariate.

**Targeted data analysis.** Differences in metabolite mean concentrations were assessed using t-tests with Benjamini-Hochberg false discovery rate (FDR) correction with a  $q = 0.2$  [49]. The fold difference used in the oxylipin/endocannabinoid network visualizations were calculated by division of the sPTB group mean by that of the FTB group. Group means were calculated using normally distributed data. Differences in cytochrome p450 metabolites were assessed using factorial analysis with preterm status, BMI category and the preterm x BMI



interaction as fixed effects. Additionally, sPTB effect in the individual BMI categories was assessed using contrast post-test. Additional contrast post-test was applied to determine the difference between normal weight versus underweight and obese FTB groups.

**Untargeted data analysis.** Variables were clustered using SAS (Cary, NC) developed algorithm that uses principal components analysis for variable grouping and cluster components (the linear combination of all variables in each cluster) were calculated for each individual cluster to reduce the dimensionality and collinearity of the data and to gain additional information about associations among variables. Clustering resulted in combining 1194 variables into 179 clusters. Cluster components were further used in t-test analysis to describe the sPTB effect in each BMI category independently. P values from the t-tests were FDR corrected with the  $q = 0.2$ , as described above. **S3 Table** describes cluster members as well as their correlations within the cluster, least square means (standard error range) and t-test p-values for both clusters and individual metabolites.

**Predictive modeling.** Stepwise logistic regression was applied using automated process in JMP to determine the minimum strongest predictors of preterm delivery and was applied separately for each BMI category. Only quantitative data (i.e. targeted metabolomics) were used to build the models, which includes oxylipins, endocannabinoids, ceramides and bile acids to ensure the maximal translational potential of the model. Model variable addition was stopped at the minimum Bayesian Information Criterion (BIC). Models were assessed by evaluation of the area under the receiver-operator curve (ROC-AUC).

## Results

### Study cohort demographics

Among the women included in this analysis, most were Hispanic (50%) or non-Hispanic white (26%), many had greater than high school education (45%), and the mean age was 26 years. Demographics are summarized in **S4 Table**.

### Obese women experiencing sPTB show higher autoxidation and pro-inflammatory lipids

Targeted analysis detected 58 of 83 measured oxylipins, including products of cytochrome P450 (CYP), cyclooxygenase (COX), lipoxygenase (LOX), nitric oxide synthase metabolism and autoxidation, 10 of 21 endocannabinoids, and 5 of 5 PUFA (**Fig 1**). When testing for mean difference in targeted metabolites between sPTB vs FTB while using BMI as a continuous variable, only 7% had a  $p < 0.05$ , but none passed an FDR correction at  $q = 0.2$ . Of note, similar results were obtained when adjusting for BMI as a categorical rather than continuous variable. On the other hand, when using BMI categories in factorial analysis, we found significant interaction between BMI and birth categories (11% with  $p < 0.05$ ) therefore, further analysis was stratified by BMI. T-test analysis was performed separately for normal weight, obese and underweight subjects. No significant differences in oxylipins, endocannabinoids or PUFAs were detected in the normal weight women, which are thus excluded from **Fig 1**. Among obese women, sPTB was associated with higher levels of LOX and autoxidation metabolites (orange nodes in **Fig 1**), regardless of the parent fatty acid's carbon chain length and unsaturation. Although most hydroxy fatty acids (mainly LOX metabolites) are also products of autoxidation, arachidonic acid (C20:4n6—AA) derived 9-hydroxyeicosatetraenoic acid (9-HETE) and F2 isoprostanes, and eicosapentaenoic acid (C20:5n3—EPA) derived 9-hydroxyeicosapentaenoic acid (9-HEPE) are uniquely produced by autoxidation and were ~ 3 fold higher in obese sPTB subjects when compared to obese FTB subjects. Higher levels of six





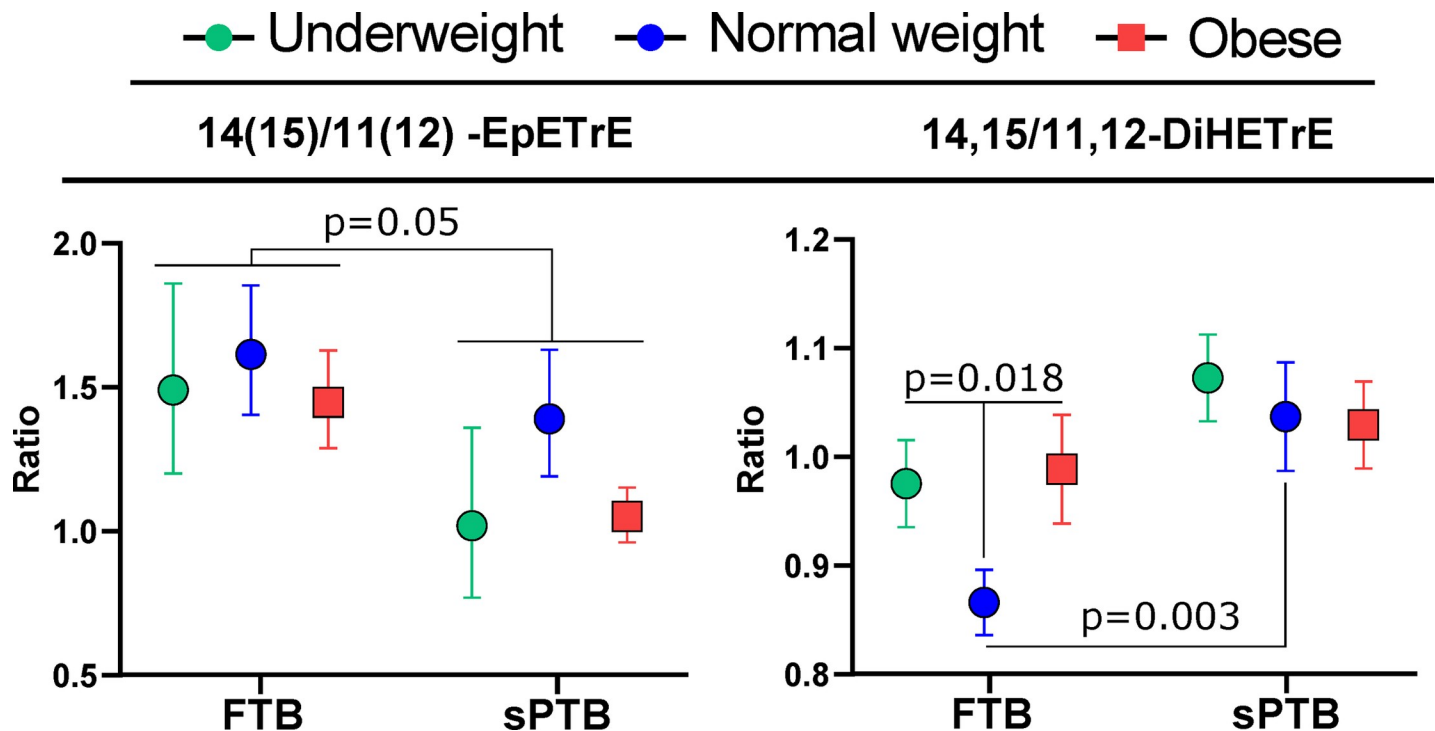


**Fig 2. Regioisomer-specific differences in arachidonic acid cytochrome p450 (CYP) metabolism.** Ratios of arachidonic acid CYP metabolite regioisomers (EpETrEs) and their soluble epoxide hydrolase (sEH)-dependent metabolites (DiHETrEs) stratified by BMI category and delivery group (sPTB and FTB). The regioisomeric ratios were calculated by dividing the concentrations of 14(15)-EpETrE or 14,15-DiHETrE by the concentration of 11(12)-EpETrE or 11,12-DiHETrE for epoxides and diols, respectively. The 14(15)/11(12)-EpETrE birth group effect was generated by a factorial analysis with BMI category, delivery group and the delivery x BMI interaction as fixed effects, and no significant interactions were detected. For the 14,15/11,12-DiHETrE ratio comparisons, the two p values reflect 1) the difference between FTB normal weight vs FTB obese and underweight, and 2) the difference between normal weight FTB vs normal weight sPTB. Error bars represent standard error. N = 17 per group. Point color: green—underweight; blue—normal weight; red—obese. EpETrE—epoxyeicosatrienoic acid; DiHETrE—dihydroxyeicosatrienoic acid.

<https://doi.org/10.1371/journal.pone.0239115.g002>

( $p = 0.018$ ). The same behavior was observed for the ratio of 14,15- to 8,9-DiHETrE (S1 Fig). Independently, sPTB subjects had higher concentration of 11(12)-EpETrE and all AA-derived diols, when compared to FTB, in obese group only (S1 Fig).

### Both underweight and obese women who have sPTB show signs of dyslipidemia

To investigate broader metabolic perturbations in sPTB we used serum untargeted metabolomics of complex lipids and biogenic amines (Fig 3). We use variable clustering as a method of data reduction, to help summarize general differences in lipid and biogenic amines metabolism. S3 Table describes the 179 unique clusters of untargeted metabolomic features, including cluster membership, cluster correlations, means and p-values of cluster components and individual metabolites. Similar to the targeted data, when analyzing unstratified data using BMI as a continuous variable, we found only 6% of cluster components with  $p < 0.05$ , but none passed an FDR correction at  $q = 0.2$ . On the other hand, when using BMI categories in factorial analysis, we found significant interaction between BMI and birth categories (10% with  $p < 0.05$ ) therefore, the further analysis was stratified by BMI. Similar to the oxylipin and endocannabinoid results, the normal weight sPTB group did not display significant differences and are not displayed in Fig 3. A summary of the numbers of identified lipids within each lipid class is presented in the S5 Table.

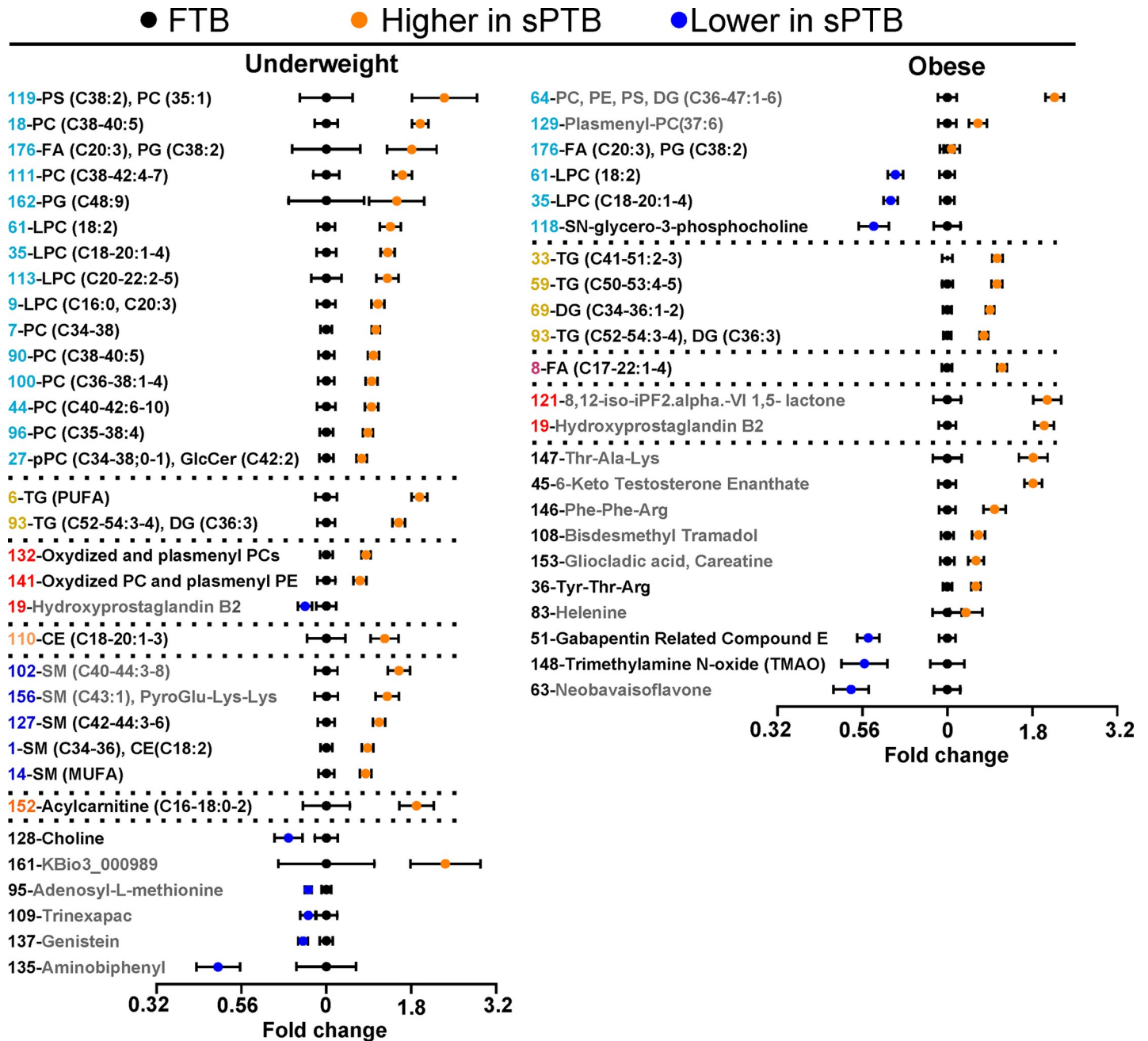


**Fig 3. Differences in complex lipids and biogenic amines between sPTB and FTB deliveries.** Results of the t-test analysis performed on variable cluster components, presented for women with underweight and obese BMI. Data are presented as the fold change from the FTB for each weight category. Each cluster is represented by a number and labeled with either a general description of variables within the cluster or the most representative metabolite. Clusters composed uniquely from metabolites identified only by parent mass (i.e. MSI level 3) are colored gray and should be interpreted with caution. A complete list of metabolites within each cluster with group means, p-values and MSI level are provided in the S3 Table. All displayed variables have  $p < 0.05$  and passed FDR correction at  $q = 0.2$ . PC-phosphatidylcholine; PE-phosphatidylethanolamine; PS-phosphatidylserine; TG-triglyceride; DG-diglyceride; CE-cholesterol ester; SM-sphingomyelin; CA-cholic acid; FA-Fatty acids. Clusters are colored according their lipid classes: phospholipids and lysophospholipids-light blue; TG-yellow; oxidized lipids-red; SM-blue; CE-light orange; FA-purple; acylcarnitine-dark orange. Description of complex lipids—(total number of fatty acids carbon atoms: total number of double bounds). Error bars represent standard error. N = 17 per group.

<https://doi.org/10.1371/journal.pone.0239115.g003>

With respect to complex lipids, differences observed between FTB and sPTB groups were unique for each BMI category, with only two commonly affected clusters, including cluster 93 (containing polyunsaturated triglycerides) and cluster 176 (containing homo- $\gamma$ -linolenic acid and phosphatidylglycerol). Both underweight and obese sPTB groups showed higher triglycerides and diglycerides (underweight group clusters—6, 93; obese group clusters—33, 59, 69, 93). As seen in Fig 4, which presents differences in individual lipids stratified by fatty acid moiety unsaturation and carbon chain length, this difference was manifested entirely in polyunsaturated species in the underweight group and showed a similar pattern in the obese group. The underweight sPTB group also showed higher levels of phospholipids and lysophospholipids (clusters 7, 9, 18, 27, 35, 44, 61, 90, 96, 100, 111, 113, 119, 162 and 176). In contrast, obese subjects experiencing sPTB had higher levels of only three phospholipid containing clusters (clusters 64, 129 and 176) and lower levels of lysophospholipids (clusters 35, 61 and 118). The differences in phospholipids did not manifest specificity towards fatty acid moiety unsaturation or chain length. Underweight subjects experiencing sPTB also displayed higher levels of sphingomyelins (clusters 1, 14, 102, 127 and 156), cholesterol esters (cluster 110) and acylcarnitines (cluster 152).

The sPTB association with oxidized lipids also differed between underweight and obese subjects. The obese sPTB group showed higher levels of F2 isoprostanes (consistent with the oxylipin analyses), while hydroxyprostaglandin B2 was lower in underweight subjects who experienced sPTB. The underweight sPTB group also showed higher levels of LA and aLA and lower levels of EPA, while obese subjects experiencing sPTB manifested higher levels of almost all fatty acids except for EPA, C14:1n5 and C14:0 and C12:0 (Fig 4). Differences in fatty acids levels observed in untargeted analysis are consistent with the targeted analyses (Fig 1).

With respect to biogenic amines, underweight sPTB group showed lower levels of choline, whereas obese sPTB subjects displayed lower levels of trimethylamine N-oxide (TMAO). Differences in sPTB were also observed among bile acids and ceramides analyzed using a targeted approach. THCSA was higher in the normal weight sPTB group (sPTB/FTB = 1.6,  $p = 0.004$ ), while the underweight sPTB group had lower DCA levels (FTB/sPTB = 3,  $p = 0.033$ ) and the obese sPTB group showed lower levels of GLCA (FTB/sPTB = 1.9,  $p = 0.023$ ). Sphingosine (C18:1) was higher in both underweight (sPTB/FTB = 1.7,  $p = 0.005$ ) and obese (sPTB/FTB = 1.8,  $p = 0.01$ ) sPTB groups.

### sEH metabolite regioisomers are predictors of sPTB in normal and underweight women

Predictive models of sPTB were developed using stepwise logistic regression analyses of targeted metabolomic data (Table 1). Similar to the t-tests, the strongest models were obtained when stratified by BMI category ( $RSq_{\text{underweight}} = 0.60$ ;  $RSq_{\text{normal weight}} = 1.0$ ;  $RSq_{\text{obese}} = 0.67$ ). Without BMI stratification a much weaker model was obtained (final model  $RSq = 0.24$ , with BMI itself not being selected by the stepwise logistic regression analysis). The elevated ratio of 14,15-/11,12-DiHETrE was selected as a factor in sPTB prediction for the underweight and normal weight, but not obese groups. Additionally, the sPTB model for normal weight subjects was characterized by a lower 12,13-/9,10-dihydroxy-octadeca(mono)enoic acid (DiHOME) ratio (i.e. the LA analogs of DiHETrEs) and a higher 14(15)-EpETrE/14,15-DiHETrE ratio. On the other hand, the sPTB in the obese group was best predicted by elevated levels of oleoylethanolamide (OEA), 5,6-DiHETrE and 6-trans-leukotriene B4 (6-trans-LTB4).

## Discussion

Preterm birth can lead to lifelong adverse health consequences and places significant strain on individuals, their families and the health care system. While our understanding of factors

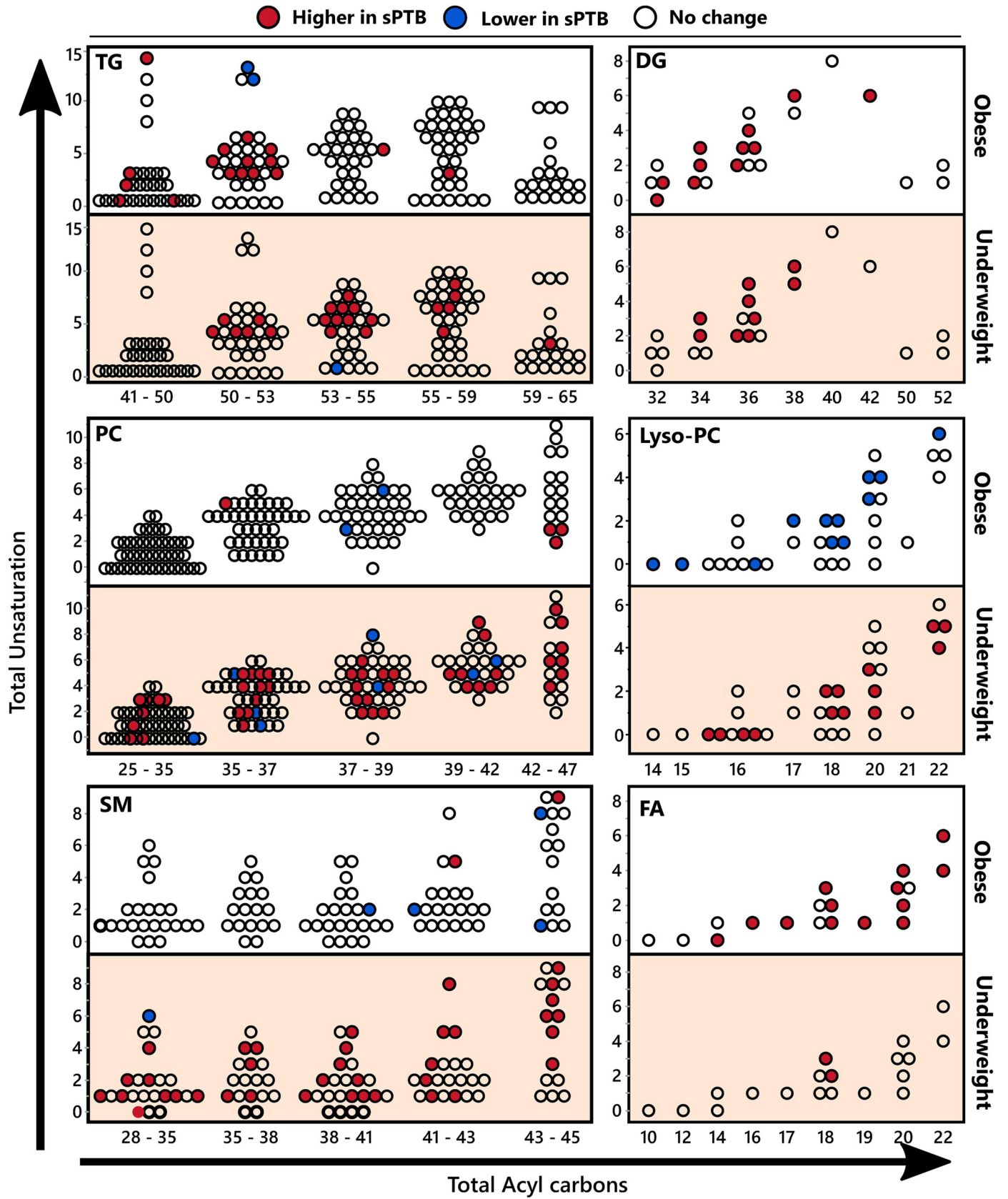


**Fig 4. Serum complex lipids stratified by acyl chain length and number of double bonds.** Differences in serum complex lipids between birth categories in obese and underweight women, stratified by acyl chain length and number of double bonds. Dots represent complex lipid species, and are positioned according to the total acyl chain unsaturation (y axis) and the total acyl chain length (x axis). Colors indicate significance and directionality of compared means (t-test  $p < 0.05$ ): red—higher in sPTB, blue—lower in sPTB, white—no change. TG—triglyceride; DG—diglyceride PS—phosphatidylserine; SM—sphingomyelin; FA—fatty acids. The number of detected individual complex lipids and the number of differences between sPTB and FTB for each chemical class are summarized in [S5 Table](#). Means of individual lipids and corresponding p-values are provided in [S3 Table](#).

<https://doi.org/10.1371/journal.pone.0239115.g004>

leading to this condition are still emerging [2], the early identification of subjects at elevated risk for sPTB offers opportunities to improve therapeutic strategies and enhance clinical outcomes. Body mass index either above ( $>30 \text{ kg/m}^2$ ) or below ( $<18.5 \text{ kg/m}^2$ ) the normal range increases the risk of sPTB [12–16], therefore the current study was designed to identify metabolic perturbations present in serum at mid-gestation that are associated with sPTB in women of low and high BMI. Findings highlight sPTB risk as a complex metabolic phenomenon that is influenced by BMI.

Inflammation is an important component of sPTB [16, 19–21], and many mediators of inflammation are known including oxylipins, endocannabinoids and bile acids. Oxylipins constitute a metabolite superclass formed by coordinated metabolic cascades with important inflammatory and immunomodulatory functions [50]. COXs lead to prostanoid and thromboid synthesis, LOXs produce hydroperoxides leading to an array of downstream products (e.g. mid-chain alcohols, ketones, leukotrienes, lipoxins, resolvins), and CYPs form epoxy and omega-hydroxy fatty acids, while sources of reactive oxygen species (e.g. NADPH oxidases, mitochondria, peroxisomes, environmental pollutants) lead to PUFA autooxidation producing racemic peroxide-associated products including alcohols and prostaglandins [51–53]. In general, prostanoids have both pro- and anti-inflammatory roles [54], epoxy fatty acids are anti-inflammatory, suppressing pro-inflammatory cytokine production [55], while mid-chain alcohols are pro-inflammatory and can induce pro-inflammatory cytokines [63, 64]. The acylethanolamides, which include a major class of endogenous cannabinoid receptor and peroxisome proliferator-activated receptor alpha (PPAR $\alpha$ ) ligands, also modulate inflammation, and have circulating concentrations that are modulated by acute inflammatory responses [56]. Notably, both underweight and obese women who experienced sPTB showed distinct oxylipin and

**Table 1. Prediction of preterm delivery using serum lipid mediators.**

BMI	Step	Parameter	p-value	sPTB/FTB	RSq	BIC	ROC AUC
Underweight	1	18:1 Sphingosine	0.0094	+	<b>0.143</b>	47.4	0.77
	2	14,15/11,12-DiHETrE	0.0332	+	<b>0.239</b>	46.4	0.79
	3	1/2_AG	0.0103	+	<b>0.379</b>	43.4	0.87
	4	Ceramide (d40:2)	0.0012	-	<b>0.601</b>	36.4	0.97
Normal weight	1	14,15/11,12-DiHETrE	0.0016	+	<b>0.218</b>	42.8	0.81
	2	12,13/9,10-DiHOME	0.0169	-	<b>0.343</b>	40.6	0.87
	3	THCSA	0.0017	+	<b>0.558</b>	34.2	0.94
	4	14(15)-EpETrE/DiHETrE	0	+	<b>1</b>	17.5	1.00
Obese	1	OEA	0	+	<b>0.367</b>	36.9	0.87
	2	5,6-DiHETrE	0.007	+	<b>0.522</b>	33.1	0.92
	3	6-trans LTB4	0.0094	+	<b>0.665</b>	29.9	0.97

Prediction of preterm delivery using serum levels of oxylipins, sphingolipids and ceramides, stratified by the BMI category. Stepwise logistic regression model (left side) shows the order of metabolites entered into the model. The “+” and “-” indicate the directionality of differences of means metabolite values observed between the birth categories. The model was stopped when the addition of next parameter would result in increase in corrected Bayesian Information Criterion (BIC). Receiver operating characteristic area under the curve (ROC AUC) is shown for each step of the model.

<https://doi.org/10.1371/journal.pone.0239115.t001>



endocannabinoid levels at mid-gestation, while women in the normal weight women manifested fewer sPTB-associated metabolomic excursions.

While obesity can directly influence the circulating metabolome, if these changes are themselves important factors in sPTB risk, an exacerbation of these effects would be expected in the obese sPTB group. In fact, elevated fatty acid ethanolamides and reduced lysophosphatidylcholines with unchanged levels of phosphatidylcholines are the features observed in obesity [63, 64], the same changes were found by us to be exacerbated in the obese sPTB group. Moreover, the obese sPTB group showed higher levels of PUFA mono-alcohols than the obese FTB group, including the autoxidation products 9-HETE and F2-isoprostanes. All detected mono-alcohols, non-vicinal diols (e.g. leukotrienes) and triols (e.g. lipoxins) correlated strongly with the autooxidative markers (S6 Table) supporting an autooxidative origin [57, 58]. A recent study of effects of long-term storage on the plasma metabolome reports general stability for up to 7yrs, with significant changes observed with additional time up to 16yrs [59]. Moreover, both preanalytical handling of the samples, and long-term storage prior to analysis can increase fatty acids alcohols and isoprostanes [60, 61], and it is possible that observed changes in autoxidation markers are not biological. With respect to oxylipins, stability for up to 15 months has been reported [62], but longer duration influences have not been reported. However, exploration of archived plasma has proven useful for oxylipin discovery efforts identifying metabolites with correlations to known inflammatory markers [63]. Therefore, we cannot explicitly confirm that lipid markers identified here were not artifactually generated, however, as the samples were selected at random with no difference in collection time between groups, we expect this to contribute to random error but not biased the results. Moreover, our findings are consistent with a recently published analysis of eicosanoids in subjects experiencing sPTB [27] also using samples stored for a prolonged period of time prior to analysis. Those findings indicate that obese individuals either experience oxidative stress, or their plasma lipids are more susceptible to oxidation, at mid-gestation, consistent with previous reports regarding obesity-associated oxidative stress [64], and the elevated production of PUFA mono-alcohols in obesity-associated disorders [37, 65]. Notably, both targeted and untargeted metabolomics showed higher levels of non-esterified fatty acids in the obese sPTB group, further supporting dyslipidemia and adipose tissue insulin resistance in these individuals [66]. Together, these findings are consistent with poorer metabolic health characterized by exacerbated mid-gestation dyslipidemia in obese women who experience sPTB relative to those obese women who deliver at term.

Underweight women who experienced sPTB also manifested signs of dyslipidemia but not oxidative stress. The underweight sPTB group had higher non-esterified 18 carbon PUFAs and lower EPA, along with higher levels of most complex lipid species. In particular, the majority of detected phospholipids were elevated, a change associated with insulin resistance in young adults [17]. While lipoprotein speciation was not directly measured, the elevated levels of triglycerides with strong correlations to phosphatidylcholine levels are consistent with increased very low density lipoprotein levels [67]. Beyond these findings, the underweight sPTB subjects also showed higher levels of long-chain acylcarnitines including AC18:1, AC18:2 and AC16:0 which have been reported to be increased in obese and diabetic subjects [68]. Moreover, as serum AC16:0 and AC18:1 are reported to be positively correlated with TNF $\alpha$  and IL-6 and associated with fatty liver disease [69], these changes may indicate inflammation and poor metabolic health in the underweight women. Changes observed in bile acids metabolism were also consistent with body weight associated changes [70]. Therefore, underweight women who experience sPTB also show signs of dyslipidemia that are distinct from the sPTB characteristics of the obese subjects.

While differences were seen between the obese and underweight sPTB groups, similarities were also noted. For instance, women who were underweight or obese and experienced sPTB

both displayed specific enrichment in triglyceride species carrying polyunsaturated fatty acids. Dyslipidemia was previously described as a sPTB risk factor [71, 72]. Moreover, 15-keto-PGE2 was one of the few oxylipins with higher levels in both obese and underweight sPTB groups. This oxylipin is derived from PGE2 [73] and catabolized by prostaglandin reductase 2 [74]. 15-Keto PGE2 is an important PPAR $\gamma$  agonist during adipocyte differentiation [74]. PPAR $\gamma$  also regulates intracellular lipolysis in adipose tissue [75], and activated adipose PPAR $\gamma$  could explain the elevated free fatty acids in sPTB subjects. On the other hand, 15-Keto PGE2 was positively associated with better LPS-induced sepsis survival and the suppression of pro-inflammatory cytokines production in murine macrophages [76]. Since sPTB was associated with elevated levels of circulating pro-inflammatory cytokines, the increased 15-Keto PGE2 is consistent with a modulating anti-inflammatory response at mid-gestation. An immunosuppressive role of prostaglandins in inflammation resolution was previously reported [54]. Therefore, activation of the immune system including both the pro- and anti-inflammatory tones, are associated with sPTB risk in a weight independent fashion.

While few metabolites discriminated sPTB from FTB in normal weight individuals, those that did suggested subtle changes in mid-gestation CYP/sEH epoxy fatty acid metabolism resulting in shifted regioisomeric metabolite profiles. Notably, these isomeric shifts were consistent in both underweight and obese FTB women, when compared to the normal weight women, supporting a common shift in CYP/sEH epoxy fatty acid metabolism at the both extremes of BMI, groups that are at higher risk for sPTB. Epoxy fatty acids are generated by multiple CYP enzymes and are further converted to their corresponding vicinal diols by epoxide hydrolases [77, 78]. While CYP and epoxide hydrolases show some regioselective product formation and substrate selective respectively, isomeric changes in CYP metabolite profiles in circulation are poorly characterized and not yet associated with specific metabolic outcomes. However here, in the normal weight sPTB group we found a preferential production of the arachidonic acid-derived 14,15-DiHETrE over the 11,12- and 8,9-regioisomers, accompanied by a decrease in the ratio of 14(15)-/11(12)-EpETrE, precursors of the corresponding diols. Relative changes in individual EpETrEs were not significant. In fact, the 14,15-/11,12-DiHETrE ratio was a strong predictor of sPTB in normal weight and to a lesser extent in underweight subjects. These findings are consistent with the reported elevation of 11(12)-EpETrE, but not 14(15)-EpETrE in sPTB [27]. Additionally, the fact that normal weight subjects experiencing FTB had lower ratios of 14,15-/11,12-DiHETrE and 14,15-/8,9-DiHETrE than both the underweight and obese FTB groups suggests that body mass either modulates or masks the underlying biochemistry. Interestingly, the ratio of 14,15-/11,12-DiHETrE in ovarian follicular fluid was previously shown to be tightly correlated with plasma estradiol levels across the estrus cycle in the pig [79], and elevated plasma and amniotic estradiol is associated with sPTB in women [80], fostering a speculated connection between CYP metabolism, steroid hormone production and sPTB. Along these lines, several reports also suggest the involvement of epoxy fatty acids in the regulation of matrix metalloproteinases (MMPs) [81, 82]. MMPs are crucial for membrane rupture during delivery [83] and dysregulation of their expression was reported in sPTB [84]. Therefore, the potential connection between dysregulation of CYP metabolism, MMP and sPTB are intriguing in light of our observation of isomeric shifts in arachidonic acid-derived CYP metabolites. Understanding the sources of the observed alteration in DiHETrE regioisomeric abundance may provide novel approaches to reduce the risk of sPTB in the future.

This was a small study conducted using biobanked aliquots of collected serum samples collected at one timepoint in pregnancy, which have inherent limitations. As such, factors including fasting state and pre-analytical sample handling were not explicitly controlled. However, in our previous study simulating preanalytical sample handling of serum from the biobank used

here, with the exception of lysophospholipids, all compounds described here as associated with sPTB were not affected [60]. Additionally, we have no reason to expect that sample handling would have differed between those women who experienced sPTB versus FTB, given that samples were collected prospectively, before the window of delivery of a liveborn infant. Additionally, due to the limitation in available samples, the range of gestational age in underweight sPTB group was broader than in obese and normal weight sPTB groups. The small group size precluded the robust validation of the reported predictive models, and our findings require validation in independent cohorts. Thus, the results should be applied elsewhere cautiously until such validation has been completed.

In summary, our results show distinct metabolic manifestations of the sPTB phenotype depending on the BMI category and provides further evidence for inflammatory and autooxidative origin of this phenomenon. More importantly, this work demonstrated the potential to predict sPTB at midterm using new set of metabolomic markers and stratification by BMI. This would be especially important for the mothers without weight related risk factors. Moreover, our findings point towards the potential role of a regioisomeric shift in CYP/epoxide hydrolase-dependent AA metabolism in sPTB risk. The regioisomeric shifts in this pathway have been rarely reported and are poorly understood and to our knowledge, not yet associated with any biological phenomenon. Finally, this study opens the door to further research on the role of CYP/epoxide hydrolase metabolism in sPTB which may involve steroid hormone and MMP metabolism.

## Supporting information

**S1 Fig. Differences in serum cytochrome P450 (CYP) metabolism between preterm birth (PTB) and full-term birth (FTB) women, stratified by the BMI categories.**  
(TIF)

**S1 Table. Concentration of surrogates in surrogate spike solution.**  
(XLSX)

**S2 Table. Targeted data quantification table.**  
(XLSX)

**S3 Table. Untargeted data quantification table.**  
(XLSX)

**S4 Table. Demographic representation of experimental groups.**  
(DOCX)

**S5 Table. Number of detected individual complex lipids and the number of differences between sPTB and FTB for each chemical class.**  
(DOCX)

**S6 Table. Spearman's  $\rho$  correlations between non-vicinal diol (5,15-DiHETE), mono-alcohols derived from 15 and 12 LOX (15-HETE and 12-HETE respectively), leukotriene B4 (LTB4), lipoxin A4 (Variable column) and autoxidative markers, F2 isoprostanes and 9-HETE (By variable column).**  
(DOCX)

## Acknowledgments

The biospecimens and data used in this study were obtained from the California Biobank Program (SIS request number 637).

**Disclaimer:** The California Department of Public Health is not responsible for the results or conclusions drawn the authors of this publication.

## Author Contributions

**Conceptualization:** Nima Aghaeepour, David K. Stevenson, Gary M. Shaw, Suzan L. Carmichael.

**Data curation:** Kamil Borkowski, John W. Newman, Jonathan A. Mayo, Ivana Blazenović.

**Formal analysis:** Kamil Borkowski, Jonathan A. Mayo, Ivana Blazenović, David K. Stevenson, Gary M. Shaw, Suzan L. Carmichael.

**Funding acquisition:** John W. Newman, Oliver Fiehn.

**Investigation:** Kamil Borkowski, John W. Newman, Jonathan A. Mayo, Ivana Blazenović, David K. Stevenson, Gary M. Shaw, Suzan L. Carmichael.

**Methodology:** Kamil Borkowski.

**Project administration:** Kamil Borkowski, John W. Newman, David K. Stevenson, Gary M. Shaw, Suzan L. Carmichael.

**Resources:** John W. Newman, Oliver Fiehn, David K. Stevenson, Gary M. Shaw, Suzan L. Carmichael.

**Supervision:** John W. Newman, Oliver Fiehn, David K. Stevenson, Gary M. Shaw, Suzan L. Carmichael.

**Validation:** Kamil Borkowski, John W. Newman.

**Visualization:** Kamil Borkowski, John W. Newman.

**Writing – original draft:** Kamil Borkowski, John W. Newman, David K. Stevenson, Gary M. Shaw, Suzan L. Carmichael.

**Writing – review & editing:** Kamil Borkowski, John W. Newman, Nima Aghaeepour, Oliver Fiehn, David K. Stevenson, Gary M. Shaw, Suzan L. Carmichael.

## References

1. Boyle A.K., et al., Preterm birth: Inflammation, fetal injury and treatment strategies. *J Reprod Immunol*, 2017. 119: p. 62–66. <https://doi.org/10.1016/j.jri.2016.11.008> PMID: 28122664
2. Di Renzo G.C., Tosto V., and Giardina I., The biological basis and prevention of preterm birth. *Best Pract Res Clin Obstet Gynaecol*, 2018. 52: p. 13–22. <https://doi.org/10.1016/j.bpobgyn.2018.01.022> PMID: 29703554
3. Menon R., Spontaneous preterm birth, a clinical dilemma: Etiologic, pathophysiologic and genetic heterogeneities and racial disparity. *Acta Obstetrica et Gynecologica Scandinavica*, 2008. 87(6): p. 590–600. <https://doi.org/10.1080/00016340802005126> PMID: 18568457
4. Cappelletti M., et al., Inflammation and preterm birth. *J Leukoc Biol*, 2016. 99(1): p. 67–78. <https://doi.org/10.1189/jlb.3MR0615-272RR> PMID: 26538528
5. Gilman-Sachs A., et al., Inflammation induced preterm labor and birth. *J Reprod Immunol*, 2018. 129: p. 53–58. <https://doi.org/10.1016/j.jri.2018.06.029> PMID: 30025845
6. Helmo F.R., et al., Intrauterine infection, immune system and premature birth. *J Matern Fetal Neonatal Med*, 2018. 31(9): p. 1227–1233. <https://doi.org/10.1080/14767058.2017.1311318> PMID: 28423971
7. Deressa A.T., et al., Factors associated with spontaneous preterm birth in Addis Ababa public hospitals, Ethiopia: cross sectional study. *BMC Pregnancy Childbirth*, 2018. 18(1): p. 332. <https://doi.org/10.1186/s12884-018-1957-0> PMID: 30103704
8. Pandey M., Chauhan M., and Awasthi S., Interplay of cytokines in preterm birth. *Indian J Med Res*, 2017. 146(3): p. 316–327. [https://doi.org/10.4103/ijmr.IJMR\\_1624\\_14](https://doi.org/10.4103/ijmr.IJMR_1624_14) PMID: 29355137

9. Wei S.Q., Fraser W., and Luo Z.C., Inflammatory cytokines and spontaneous preterm birth in asymptomatic women: a systematic review. *Obstet Gynecol*, 2010. 116(2 Pt 1): p. 393–401. <https://doi.org/10.1097/AOG.0b013e3181e6dbc0> PMID: 20664401
10. Raba G. and Tabarkiewicz J., Cytokines in Preterm Delivery: Proposal of a New Diagnostic Algorithm. *J Immunol Res*, 2018. 2018: p. 8073476. <https://doi.org/10.1155/2018/8073476> PMID: 29850638
11. Jelliffe-Pawlowski L.L., et al., Combined elevated midpregnancy tumor necrosis factor alpha and hyperlipidemia in pregnancies resulting in early preterm birth. *Am J Obstet Gynecol*, 2014. 211(2): p. 141 e1–9.
12. Vinturache A., et al., Maternal body mass index and the prevalence of spontaneous and elective preterm deliveries in an Irish obstetric population: a retrospective cohort study. *BMJ Open*, 2017. 7(10): p. e015258. <https://doi.org/10.1136/bmjopen-2016-015258> PMID: 29038176
13. Kosa J.L., et al., The association between pre-pregnancy BMI and preterm delivery in a diverse southern California population of working women. *Matern Child Health J*, 2011. 15(6): p. 772–81. <https://doi.org/10.1007/s10995-010-0633-4> PMID: 20602159
14. Dekker G.A., et al., Risk factors for preterm birth in an international prospective cohort of nulliparous women. *PLoS One*, 2012. 7(7): p. e39154. <https://doi.org/10.1371/journal.pone.0039154> PMID: 22815699
15. Shaw G.M., et al., Maternal prepregnancy body mass index and risk of spontaneous preterm birth. *Paediatr Perinat Epidemiol*, 2014. 28(4): p. 302–11. <https://doi.org/10.1111/pepe.12125> PMID: 24810721
16. Wallenstein M.B., et al., Inflammatory biomarkers and spontaneous preterm birth among obese women. *Journal of Maternal-Fetal & Neonatal Medicine*, 2016. 29(20): p. 3317–3322.
17. Kahraman S., et al., U-shaped association of body mass index with inflammation and atherosclerosis in hemodialysis patients. *J Ren Nutr*, 2005. 15(4): p. 377–86. <https://doi.org/10.1053/j.jrn.2005.07.004> PMID: 16198930
18. Liston A., Carr E.J., and Linterman M.A., Shaping Variation in the Human Immune System. *Trends in Immunology*, 2016. 37(10): p. 637–646. <https://doi.org/10.1016/j.it.2016.08.002> PMID: 27692231
19. Vadillo-Ortega F. and Estrada-Gutierrez G., Role of matrix metalloproteinases in preterm labour. *BJOG*, 2005. 112 Suppl 1: p. 19–22.
20. Sundrani D., et al., Investigating the expression of MMPs and TIMPs in preterm placenta and role of CpG methylation in regulating MMP-9 expression. *IUBMB Life*, 2017. 69(12): p. 985–993. <https://doi.org/10.1002/iub.1687> PMID: 29130646
21. Velez D.R., et al., Preterm birth in Caucasians is associated with coagulation and inflammation pathway gene variants. *PLoS One*, 2008. 3(9): p. e3283. <https://doi.org/10.1371/journal.pone.0003283> PMID: 18818748
22. Karakas S.E., et al., Changes in plasma metabolites and glucose homeostasis during omega-3 polyunsaturated fatty acid supplementation in women with polycystic ovary syndrome. *BBA Clin*, 2016. 5: p. 179–85. <https://doi.org/10.1016/j.bbacli.2016.04.003> PMID: 27182493
23. Grapov D., et al., Exercise plasma metabolomics and xenometabolomics in obese, sedentary, insulin-resistant women: impact of a fitness and weight loss intervention. *Am J Physiol Endocrinol Metab*, 2019. 317(6): p. E999–E1014. <https://doi.org/10.1152/ajpendo.00091.2019> PMID: 31526287
24. Borkowski K., et al., Walnuts change lipoprotein composition suppressing TNFalpha-stimulated cytokine production by diabetic adipocyte. *J Nutr Biochem*, 2019. 68: p. 51–58. <https://doi.org/10.1016/j.jnutbio.2019.03.004> PMID: 31030167
25. Rajamani A., et al., Oxylipins in triglyceride-rich lipoproteins of dyslipidemic subjects promote endothelial inflammation following a high fat meal. *Sci Rep*, 2019. 9(1): p. 8655. <https://doi.org/10.1038/s41598-019-45005-5> PMID: 31209255
26. Gil A.M. and Duarte D., Biofluid Metabolomics in Preterm Birth Research. *Reproductive Sciences*, 2018. 25(7): p. 967–977. <https://doi.org/10.1177/1933719118756748> PMID: 29439621
27. Aung M.T., et al., Prediction and associations of preterm birth and its subtypes with eicosanoid enzymatic pathways and inflammatory markers. *Sci Rep*, 2019. 9(1): p. 17049. <https://doi.org/10.1038/s41598-019-53448-z> PMID: 31745121
28. Bachkangi P., et al., Prediction of preterm labour from a single blood test: The role of the endocannabinoid system in predicting preterm birth in high-risk women. *European Journal of Obstetrics & Gynecology and Reproductive Biology*, 2019. 243: p. 1–6.
29. Peiris H.N., et al., Review: Eicosanoids in preterm labor and delivery: Potential roles of exosomes in eicosanoid functions. *Placenta*, 2017. 54: p. 95–103. <https://doi.org/10.1016/j.placenta.2016.12.013> PMID: 27988062
30. Menon R., et al., Amniotic Fluid Eicosanoids in Preterm and Term Births: Effects of Risk Factors for Spontaneous Preterm Labor. *Obstetrics & Gynecology*, 2011. 118(1): p. 121–134.



31. Ovadia C., et al., Association of adverse perinatal outcomes of intrahepatic cholestasis of pregnancy with biochemical markers: results of aggregate and individual patient data meta-analyses. *Lancet*, 2019. 393(10174): p. 899–909. [https://doi.org/10.1016/S0140-6736\(18\)31877-4](https://doi.org/10.1016/S0140-6736(18)31877-4) PMID: 30773280
32. Kondrackiene J., et al., Predictors of premature delivery in patients with intrahepatic cholestasis of pregnancy. *World Journal of Gastroenterology*, 2007. 13(46).
33. Dobierzewska A., et al., Plasma cross-gestational sphingolipidomic analyses reveal potential first trimester biomarkers of preeclampsia. *PLoS One*, 2017. 12(4): p. e0175118. <https://doi.org/10.1371/journal.pone.0175118> PMID: 28384202
34. Prinz P., et al., Plasma bile acids show a positive correlation with body mass index and are negatively associated with cognitive restraint of eating in obese patients. *Frontiers in Neuroscience*, 2015. 9.
35. Tomkin G.H. and Owens D., Obesity diabetes and the role of bile acids in metabolism. *J Transl Int Med*, 2016. 4(2): p. 73–80. <https://doi.org/10.1515/jtim-2016-0018> PMID: 28191525
36. Sokolowska E. and Blachnio-Zabielska A., The Role of Ceramides in Insulin Resistance. *Frontiers in Endocrinology*, 2019. 10.
37. Grapov D., et al., Type 2 diabetes associated changes in the plasma non-esterified fatty acids, oxylipins and endocannabinoids. *PLoS One*, 2012. 7(11): p. e48852. <https://doi.org/10.1371/journal.pone.0048852> PMID: 23144998
38. Headen I., et al., The accuracy of self-reported pregnancy-related weight: a systematic review. *Obes Rev*, 2017. 18(3): p. 350–369. <https://doi.org/10.1111/obr.12486> PMID: 28170169
39. Pedersen T.L. and Newman J.W., Establishing and Performing Targeted Multi-residue Analysis for Lipid Mediators and Fatty Acids in Small Clinical Plasma Samples. *Methods Mol Biol*, 2018. 1730: p. 175–212. [https://doi.org/10.1007/978-1-4939-7592-1\\_13](https://doi.org/10.1007/978-1-4939-7592-1_13) PMID: 29363074
40. Smedes F., Determination of total lipid using non-chlorinated solvents. *Analyst*, 1999. 124: p. 1711–1718.
41. Midtbo L.K., et al., Intake of farmed Atlantic salmon fed soybean oil increases hepatic levels of arachidonic acid-derived oxylipins and ceramides in mice. *J Nutr Biochem*, 2015. 26(6): p. 585–95. <https://doi.org/10.1016/j.jnutbio.2014.12.005> PMID: 25776459
42. Agrawal K., et al., Sweat lipid mediator profiling: a noninvasive approach for cutaneous research. *J Lipid Res*, 2017. 58(1): p. 188–195. <https://doi.org/10.1194/jlr.M071738> PMID: 27875258
43. Cajka T. and Fiehn O., LC-MS-Based Lipidomics and Automated Identification of Lipids Using the Lipid-Blast In-Silico MS/MS Library. *Methods Mol Biol*, 2017. 1609: p. 149–170. [https://doi.org/10.1007/978-1-4939-6996-8\\_14](https://doi.org/10.1007/978-1-4939-6996-8_14) PMID: 28660581
44. Matyash V., et al., Lipid extraction by methyl-tert-butyl ether for high-throughput lipidomics. *J Lipid Res*, 2008. 49(5): p. 1137–46. <https://doi.org/10.1194/jlr.D700041-JLR200> PMID: 18281723
45. Tsugawa H., et al., MS-DIAL: data-independent MS/MS deconvolution for comprehensive metabolome analysis. *Nat Methods*, 2015. 12(6): p. 523–6. <https://doi.org/10.1038/nmeth.3393> PMID: 25938372
46. Schymanski E.L., et al., Identifying small molecules via high resolution mass spectrometry: communicating confidence. *Environ Sci Technol*, 2014. 48(4): p. 2097–8. <https://doi.org/10.1021/es5002105> PMID: 24476540
47. Cajka T., Smilowitz J.T., and Fiehn O., Validating Quantitative Untargeted Lipidomics Across Nine Liquid Chromatography-High-Resolution Mass Spectrometry Platforms. *Anal Chem*, 2017. 89(22): p. 12360–12368. <https://doi.org/10.1021/acs.analchem.7b03404> PMID: 29064229
48. Kind T. and Fiehn O., Seven Golden Rules for heuristic filtering of molecular formulas obtained by accurate mass spectrometry. *BMC Bioinformatics*, 2007. 8: p. 105. <https://doi.org/10.1186/1471-2105-8-105> PMID: 17389044
49. Benjamini Y. and Yekutieli D., Quantitative trait loci analysis using the false discovery rate. *Genetics*, 2005. 171(2): p. 783–789. <https://doi.org/10.1534/genetics.104.036699> PMID: 15956674
50. Gabbs M., et al., Advances in Our Understanding of Oxylipins Derived from Dietary PUFAs. *Adv Nutr*, 2015. 6(5): p. 513–40. <https://doi.org/10.3945/an.114.007732> PMID: 26374175
51. Mallat Z., et al., The relationship of hydroxyeicosatetraenoic acids and F2-isoprostanes to plaque instability in human carotid atherosclerosis. *J Clin Invest*, 1999. 103(3): p. 421–7. <https://doi.org/10.1172/JCI3985> PMID: 9927504
52. Picklo M.J. Sr. and Newman J.W., Antioxidant supplementation and obesity have independent effects on hepatic oxylipin profiles in insulin-resistant, obesity-prone rats. *Free Radic Biol Med*, 2015. 89: p. 182–91. <https://doi.org/10.1016/j.freeradbiomed.2015.07.152> PMID: 26398714
53. Phaniendra A., Jestadi D.B., and Periyasamy L., Free radicals: properties, sources, targets, and their implication in various diseases. *Indian J Clin Biochem*, 2015. 30(1): p. 11–26. <https://doi.org/10.1007/s12291-014-0446-0> PMID: 25646037

54. Newson J., et al., Inflammatory Resolution Triggers a Prolonged Phase of Immune Suppression through COX-1/mPGES-1-Derived Prostaglandin E2. *Cell Rep*, 2017. 20(13): p. 3162–3175. <https://doi.org/10.1016/j.celrep.2017.08.098> PMID: 28954232
55. Christmas P., *Role of Cytochrome P450s in Inflammation*. *Adv Pharmacol*, 2015. 74: p. 163–92. <https://doi.org/10.1016/bs.apha.2015.03.005> PMID: 26233907
56. Willenberg I., et al., Characterization of changes in plasma and tissue oxylipin levels in LPS and CLP induced murine sepsis. *Inflamm Res*, 2016. 65(2): p. 133–42. <https://doi.org/10.1007/s00011-015-0897-7> PMID: 26645911
57. Mazaleuskaya L.L., et al., Analysis of HETEs in human whole blood by chiral UHPLC-ECAPCI/HRMS. *J Lipid Res*, 2018. 59(3): p. 564–575. <https://doi.org/10.1194/jlr.D081414> PMID: 29301865
58. Lee J.W., et al., UPLC-MS/MS-Based Profiling of Eicosanoids in RAW264.7 Cells Treated with Lipopolysaccharide. *Int J Mol Sci*, 2016. 17(4): p. 508. <https://doi.org/10.3390/ijms17040508> PMID: 27058537
59. Wagner-Golbs A., et al., Effects of Long-Term Storage at -80 degrees C on the Human Plasma Metabolome. *Metabolites*, 2019. 9(5).
60. La Frano M.R., et al., Impact of post-collection freezing delay on the reliability of serum metabolomics in samples reflecting the California mid-term pregnancy biobank. *Metabolomics*, 2018. 14(11): p. 151. <https://doi.org/10.1007/s11306-018-1450-9> PMID: 30830400
61. Gladine C., et al., MS-based targeted metabolomics of eicosanoids and other oxylipins: Analytical and inter-individual variabilities. *Free Radic Biol Med*, 2019. 144: p. 72–89. <https://doi.org/10.1016/j.freeradbiomed.2019.05.012> PMID: 31085232
62. Koch E., et al., Stability of oxylipins during plasma generation and long-term storage. *Talanta*, 2020. 217: p. 121074. <https://doi.org/10.1016/j.talanta.2020.121074> PMID: 32498891
63. Watrous J.D., et al., Directed Non-targeted Mass Spectrometry and Chemical Networking for Discovery of Eicosanoids and Related Oxylipins. *Cell Chem Biol*, 2019. 26(3): p. 433–442 e4. <https://doi.org/10.1016/j.chembiol.2018.11.015> PMID: 30661990
64. Fernandez-Sanchez A., et al., Inflammation, oxidative stress, and obesity. *Int J Mol Sci*, 2011. 12(5): p. 3117–32. <https://doi.org/10.3390/ijms12053117> PMID: 21686173
65. Shearer G.C., et al., Abnormal lipoprotein oxylipins in metabolic syndrome and partial correction by omega-3 fatty acids. *Prostaglandins Leukot Essent Fatty Acids*, 2018. 128: p. 1–10. <https://doi.org/10.1016/j.plefa.2017.10.006> PMID: 29413356
66. Kaviarasan S., et al., F(2)-isoprostanes as novel biomarkers for type 2 diabetes: a review. *J Clin Biochem Nutr*, 2009. 45(1): p. 1–8. <https://doi.org/10.3164/jcbn.08-266> PMID: 19590700
67. Feingold, K.R. and C. Grunfeld, *Introduction to Lipids and Lipoproteins*, in *Endotext*, K.R. Feingold, et al., Editors. 2000: South Dartmouth (MA).
68. Mihalik S.J., et al., Increased levels of plasma acylcarnitines in obesity and type 2 diabetes and identification of a marker of glucolipototoxicity. *Obesity (Silver Spring)*, 2010. 18(9): p. 1695–700.
69. Enooku K., et al., Altered serum acylcarnitine profile is associated with the status of nonalcoholic fatty liver disease (NAFLD) and NAFLD-related hepatocellular carcinoma. *Sci Rep*, 2019. 9(1): p. 10663. <https://doi.org/10.1038/s41598-019-47216-2> PMID: 31337855
70. La Frano M.R., et al., Diet-induced obesity and weight loss alter bile acid concentrations and bile acid-sensitive gene expression in insulin target tissues of C57BL/6J mice. *Nutr Res*, 2017. 46: p. 11–21. <https://doi.org/10.1016/j.nutres.2017.07.006> PMID: 29173647
71. Smith C.J., et al., Maternal dyslipidemia and risk for preterm birth. *PLoS One*, 2018. 13(12): p. e0209579. <https://doi.org/10.1371/journal.pone.0209579> PMID: 30576377
72. Jiang S., et al., Maternal dyslipidemia during pregnancy may increase the risk of preterm birth: A meta-analysis. *Taiwan J Obstet Gynecol*, 2017. 56(1): p. 9–15. <https://doi.org/10.1016/j.tjog.2016.07.012> PMID: 28254234
73. Ricciotti E. and FitzGerald G.A., Prostaglandins and inflammation. *Arterioscler Thromb Vasc Biol*, 2011. 31(5): p. 986–1000. <https://doi.org/10.1161/ATVBAHA.110.207449> PMID: 21508345
74. Chou W.L., et al., Identification of a novel prostaglandin reductase reveals the involvement of prostaglandin E2 catabolism in regulation of peroxisome proliferator-activated receptor gamma activation. *J Biol Chem*, 2007. 282(25): p. 18162–72. <https://doi.org/10.1074/jbc.M702289200> PMID: 17449869
75. Berger J. and Moller D.E., The mechanisms of action of PPARs. *Annu Rev Med*, 2002. 53: p. 409–35. <https://doi.org/10.1146/annurev.med.53.082901.104018> PMID: 11818483
76. Chen I.J., et al., Targeting the 15-keto-PGE2-PTGR2 axis modulates systemic inflammation and survival in experimental sepsis. *Free Radic Biol Med*, 2018. 115: p. 113–126. <https://doi.org/10.1016/j.freeradbiomed.2017.11.016> PMID: 29175486

77. Spector A.A., Arachidonic acid cytochrome P450 epoxygenase pathway. *J Lipid Res*, 2009. 50 Suppl: p. S52–6.
78. Edin M.L., et al., Epoxide hydrolase 1 (EPHX1) hydrolyzes epoxyeicosanoids and impairs cardiac recovery after ischemia. *J Biol Chem*, 2018. 293(9): p. 3281–3292. <https://doi.org/10.1074/jbc.RA117.000298> PMID: 29298899
79. Newman J.W., et al., Cytochrome p450-dependent lipid metabolism in preovulatory follicles. *Endocrinology*, 2004. 145(11): p. 5097–105. <https://doi.org/10.1210/en.2004-0710> PMID: 15308618
80. Mazor M., et al., Human preterm birth is associated with systemic and local changes in progesterone/17 beta-estradiol ratios. *Am J Obstet Gynecol*, 1994. 171(1): p. 231–6. [https://doi.org/10.1016/0002-9378\(94\)90474-x](https://doi.org/10.1016/0002-9378(94)90474-x) PMID: 8030704
81. Sander A.L., et al., Soluble epoxide hydrolase disruption as therapeutic target for wound healing. *J Surg Res*, 2013. 182(2): p. 362–7. <https://doi.org/10.1016/j.jss.2012.10.034> PMID: 23122666
82. Moshal K.S., et al., Cytochrome P450 (CYP) 2J2 gene transfection attenuates MMP-9 via inhibition of NF-kappabeta in hyperhomocysteinemia. *J Cell Physiol*, 2008. 215(3): p. 771–81. <https://doi.org/10.1002/jcp.21356> PMID: 18181170
83. Weiss A., Goldman S., and Shalev E., The matrix metalloproteinases (MMPS) in the decidua and fetal membranes. *Front Biosci*, 2007. 12: p. 649–59. <https://doi.org/10.2741/2089> PMID: 17127325
84. Sundrani D., et al., Matrix metalloproteinases-2, -3 and tissue inhibitors of metalloproteinases-1, -2 in placentas from preterm pregnancies and their association with one-carbon metabolites. *Reproduction*, 2013. 145(4): p. 401–10. <https://doi.org/10.1530/REP-12-0520> PMID: 23412981